

Wavy-Shaped Cross-Sectional Deformation in Multiwalled Cylinders with Inner Stiffner

*Motohiro Sato¹⁾, Tetsuro Ikeda²⁾, Yuta Ishiwata²⁾, Sung-Jin Park³⁾
and Hiroyuki Shima⁴⁾

¹⁾ *Division of Engineering and Policy for Sustainable Environment,
Faculty of Engineering, Hokkaido University, Kita-13, Nishi-8, Kita-ku,
Sapporo, Japan*

²⁾ *Division of Engineering and Policy for Sustainable Environment,
Graduate School of Engineering, Hokkaido University, Kita-13, Nishi-8, Kita-ku,
Sapporo, Japan*

³⁾ *Department of Urban and Environment Engineering,
University of Incheon, 235, Dohwa-dong, Nam-gu, Incheon, Korea*

⁴⁾ *Department of Environmental Sciences and Interdisciplinary,
Graduate School of Medicine and Engineering, University of Yamanashi,
4-4-37, Takeda, Kofu, Yamanashi 400-8510, Japan*

¹⁾ tayu@eng.hokudai.ac.jp

ABSTRACT

We investigate the cross-sectional buckling of multi-concentric tubular nanomaterials, which are called multiwalled carbon nanotubes (MWNTs), using an analysis based on thin-shell theory. MWNTs under hydrostatic pressure experience radial buckling. As a result of this, different buckling modes are obtained depending on the inter-tube separation d as well as the number of constituent tubes N and the innermost tube diameter. All of the buckling modes are classified into two deformation phases, an elliptic deformation and wavy deformation. An important observation is the mechanical consequence of stiff core-tube insertion into the innermost hollow region of a given MWNT. The insertion results in a significant variance in the critical buckling pressure, above which the MWNT undergoes radial corrugation.

1. INTRODUCTION

Multiply-concentric tubular structures in transportation systems have supplied a demand for flow assurance under extreme environment. Widely known are pipe-in-pipe structures (Kyriakides, 2002a,b) and sandwich cylindrical shells (Han et al., 2004; Kardmateas et al., 2005), which are of great importance in the development of deepwater pipelines and risers in civil engineering. A pipe-in-pipe is composed of two concentrically mounted steel pipes with the annular space filled with either circulating

^{1),4)} Associate Professor

²⁾ Graduate Student

³⁾ Professor

hot water or thermal insulator, preventing the line blockage caused by dropping fluid temperature. A sandwichpipe is its improved version to increase the pressure capacity, consisting of two thin-wall steel pipes that sandwich a thicker and flexible material endowed with both structural strength and thermal insulation property. Applications of the two concentric tubular systems are often required to function under very high hydrostatic pressure; therefore, theoretical understanding of their mechanical stability and precise evaluation of critical buckling pressure are of major concern (Sato et al., 2007, 2008).

2. Formulation

2.1. Continuum Approximation

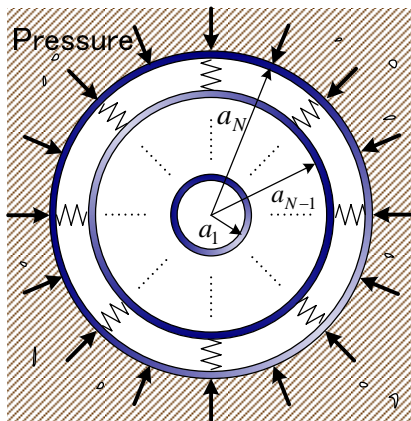


Fig.1 Illustrations of our continuum model

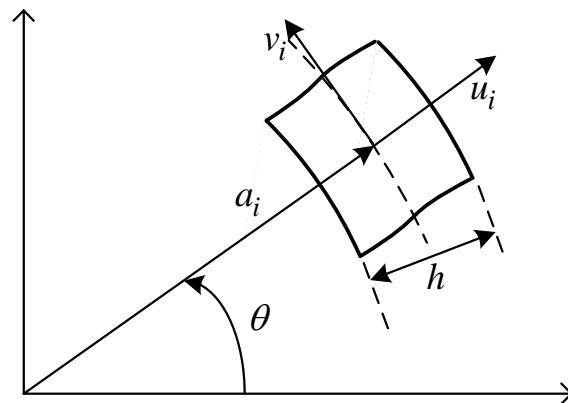


Fig.2 Element of the i th tube.

When treating many-walled nanotubes, atomistic simulations are realistic and accurate but they demand huge computational cost in general. Thus I used a simplified model based on the continuum approximation. Figure 1 shows a continuum elastic model. In the continuum approximation, the mechanical energy U of a MWCNTs per unit length in the axial direction is the sum of the deformation energy U_D of all concentric walls, the interaction energy U_I of all adjacent pairs of walls, and the potential energy Ω of the applied pressure. Thus U can be written as

$$U = U[u_i, v_i, p] = U_D + U_I + \Omega \quad (1)$$

Figure 2 shows a element that compose a nanotube. All these three energy terms are functions of and the deformation amplitudes $u_i(p, \theta)$ and $v_i(p, \theta)$ that describe the radial (r) and circumferential (θ) displacements, respectively, of the i th tube.

2.2. Energy formulation

The deformation energy U_D per axial length can be written as follows

$$U_D = \sum_{i=1}^N \frac{\alpha a_i^2}{2} \int_0^{2\pi} \left[\frac{v_i' + u_i}{a_i} + \frac{1}{2} \left(\frac{v_i - u_i'}{a_i} \right)^2 \right]^2 d\theta + \sum_{i=1}^N \frac{\beta a_i^4}{2} \left(\frac{v_i' - u_i''}{a_i^2} \right)^2 d\theta \quad (2)$$

here, α and β are written as follows

$$\alpha = \frac{Eh}{1 - \nu^2}, \quad \beta = \frac{Eh^3}{12(1 - \nu^2)} \quad (3)$$

The second term U_I in Eq. (1) is the interaction energy of all adjacent pairs of tubes described by

$$U_I = \sum_{i=1}^{N-1} \frac{c_{i,i+1} [(a_i + a_{i+1})/2]}{2} \int_0^{2\pi} (u_i - u_{i+1})^2 d\theta \quad (4)$$

Coupling coefficients c_{ij} described by

$$c_{ij} = -\frac{1}{4} \left(\frac{\partial P_{i,i+1}}{\partial h} + \frac{\partial P_{i+1,i}}{\partial h} \right) \quad (5)$$

The final term Ω in Eq. (1) is the negative of the work done by the pressure p , can be written as follows

$$\Omega = p \int_0^{2\pi} \left[u_N a_N + \frac{v_N^2 - u_N' v_N + u_N v_N' + u_N^2}{2} \right] d\theta \quad (6)$$

3. Result and Discussion

3.1. Critical pressure curve

Figure 3 shows p_c as a function of N for various values of innermost tube diameter D . Thick solid lines correspond to stiffener-induced MWNTs, while thin dashed lines the pristine MWNTs. The two insets provide enlarged views of the thin lines, making it easy to grasp the increasing behaviors of p_c with N . It follows from the figure that the inserted MWNTs give decay of $p_c(N)$ for every value of D . On the other hand, in pristine cases, the N -dependence of p_c changes dramatically with varying D ; p_c -curves show monotonic decay for small D , whereas for large D they tend to grow with N . The latter property, the growth of p_c with increasing N , is interpreted as an effective “hardening” of MWNTs, *i.e.*, the enhancement of radial stiffness of the entire MWNT by encapsulation. In contrast, decay in p_c indicates an effective “softening” of the MWNT, implying that a relatively low pressure becomes sufficient to produce radial deformation.

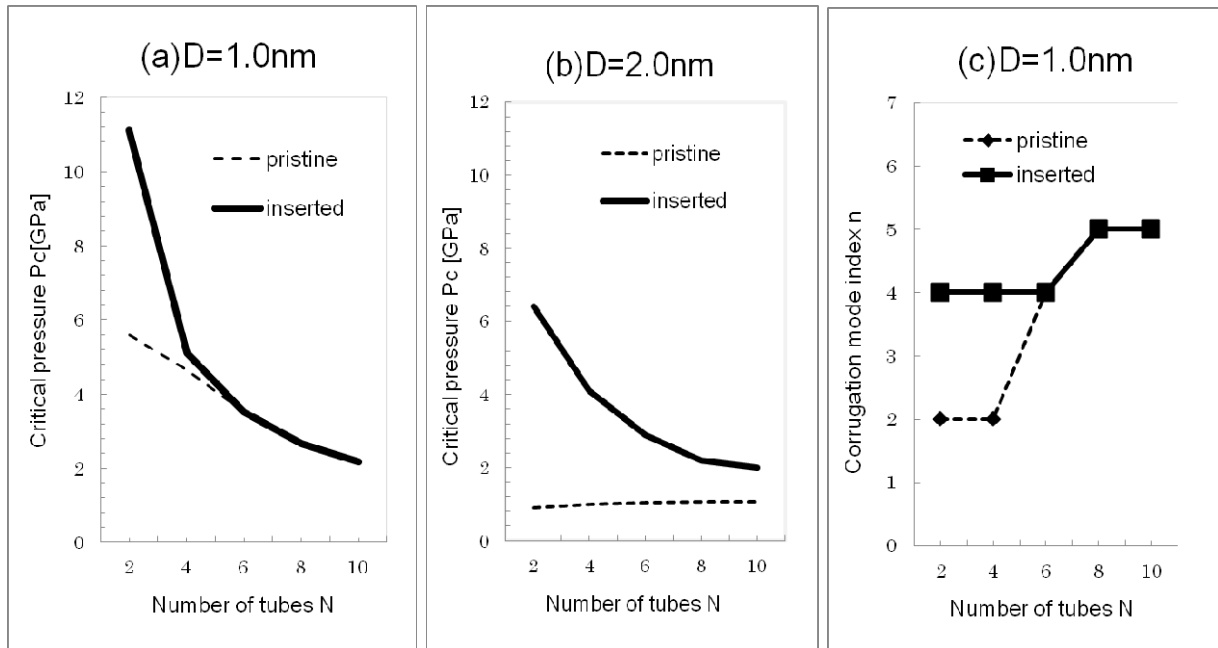


Fig.3 (a),(b): Critical pressure p_c as a function of the number of concentric tubes N .

Fig.4 (c): Radial mode index n that indicates the circumferential wave number of the deformed cross-section.

3.2. Radial corrugation emergence

Figure 4 provides the index n of radial corrugation modes observed just above p_c . We see from Fig. 4 that the deformation mode observed just above p_c jumps abruptly from $n = 2$ to $n = 4$ by stacking the concentric tubes: from $n = 4$ to $n = 6$, followed by successive emergences of higher corrugation modes with larger n (not shown). These transitions in n originate from the two competing effects inherent in MWNTs with $N \gg 1$, that is, the relative rigidity of the inner tubes and the mechanical instability of outer tubes. A large discrepancy in the radial stiffness of the inner and outer tubes gives rise to a maldistribution of the deformation amplitudes of concentric tubes interacting through the vdW forces, which consequently produces an abrupt change in the observed deformation mode at some N .

4. Summary

We have conducted the thin-shell-theory based analysis on the multiply-concentric hollow tubes in which an inner wallstiffener is inserted. As an analytical example, we focus on the buckling characteristics of MWNTs in this article. It has been found that MWNTs exhibit anomalous radial buckling behaviors under hydrostatic pressure on the order of a few GPa. An important observation in this paper is the mechanical consequence of stiff core-tube insertion into the innermost hollow region of a given MWNT. The insertion results in a significant variance in the critical buckling pressure,

above which the MWNT undergoes radial corrugation. The insertion-induced variance in the critical pressure is due to the primary role of inter-tube interaction between adjacent constituent tubes, as explained within our theoretical model.

Acknowledgment

This work was partially supported by KAKENHI (Grant-in-Aid for Young Scientists (A), No. 24686096) from MEXT, Japan.

References

- Kardmateas, G.A. and Simitzes, G.J. "Buckling of long sandwich cylindrical shells under external pressure", *J. Appl. Mech.*, **72**, 493-499.
- Kyriakides, S. (2002), "Buckle Propagation in pipe-in-pipe systems: Part I. Experiments", *Int. J. Solids Struct.*, **30**, 351-366.
- Kyriakides, S. (2002), "Buckle Propagation in pipe-in-pipe systems: Part II. Analysis", *Int. J. Solids Struct.*, **30**, 367-392.
- Park, S.J., M. Sato, T. Ikeda, H. Shima, (2012), "Hard-to-Soft Transition in Radial Buckling of Multi-Concentric Nanocylinders" *World J. Mech.*, **2**, 42-50.
- Sato, M. and Patel, M.H. (2007), "Exact and simplified estimations for elastic buckling pressures of structural pipe-in-pipe cross sections under external hydrostatic pressure", *J. Mar. Sci. Tech.*, **12**, 251-262.
- Sato, M., Patel, M.H. and Trarieux, F. (2008), "Static displacement and elastic buckling characteristics of structural pipe-in-pipe cross-sections", *Str. Eng. Mech.*, **30**, 263-278.
- Shima, H., Ghosh, S., Arroyo, M., Liboshi, K. and Sato, M. (2012), "Thin-shell theory based analysis of radially pressurized multiwall carbon nanotubes", *Comp. Mater. Sci.*, **52**, 90-94.
- Shima, H. and Sato, M. (2008), "Multiple radial corrugations in multiwall carbon nanotubes under pressure", *Nanotechnology*, **19**, 495705 (8 pages).